Form birefringence of muscle

Richard C. Haskell,* Francis D. Carlson,‡ and Paul S. Blank‡
*Department of Physics, Harvey Mudd College, Claremont, California 91711; and ‡The Thomas C. Jenkins Department of Biophysics, Johns Hopkins University, Baltimore, Maryland 21218

ABSTRACT We investigate the sensitivity of measurements of muscle birefringence to cross-bridge dynamics in the resting, active, and rigor states. The theory of form birefringence is reviewed, and an optical model is constructed for the form birefringence of muscle. Values for the parameters in the model are selected or deduced from the literature. As an illustration of the use of the model, plausible distributions for the orientations of cross-bridges in the resting, active, and rigor states are constructed using a model for cross-bridge dynamics suggested by Huxley and Kress (1985). The general magnitude of the predictions of our model is comparable with that of published measurements of muscle birefringence. However, the precise values of the predicted birefringence for the resting, active, and rigor states are sensitive to the assumed orientations of cross-bridges. We also investigate the dependence of muscle birefringence on sarcomere length and on disorder in the orientation of the myofilament array. We conclude that measurements of muscle birefringence can play a useful role in distinguishing between proposed models of cross-bridge dynamics.

I. INTRODUCTION

Several different experimental techniques have been used in the past decade in an effort to provide a description of the structural dynamics of myosin cross-bridges during muscle contraction (see review by Cooke [1986]). X-Ray studies indicate that most myosin heads are in the vicinity of the actin filaments during isometric contraction, but that no more than a third of the heads are attached to actin in a specific orientation (see overview in Huxley and Kress [1985]). Whereas the technique of x-ray scattering has yielded a great deal of structural information in relaxed and rigor muscle, the decrease in structural periodicity during contraction lessens the sensitivity of scattering patterns to the position and orientation of cross-bridges. Studies using paramagnetic and optical probes seem to be quite sensitive to the orientation of cross-bridges (see review by Thomas [1987]). However, the useful probes are extrinsic, and their use requires considerable care. Moreover the probe studies indicate significantly different values for the fraction of myosin heads attached to actin in a specific orientation during isometric contraction (20–80%) (compare Cooke et al. [1982]) with Burghardt et al. [1983]). It is clear that further experimentation is required using a variety of complementary and overlapping techniques before a consensus can be reached regarding the general structural behavior of cross-bridges during contraction.

In the present paper we examine the potential sensitivity of optical birefringence measurements to the orientation of cross-bridges in resting, active, and rigor muscle. Structural periodicity does not play a significant role in muscle birefringence; in that sense birefringence measurements have an advantage over x-ray scattering. In addition, birefringence measurements can be performed on both intact and skinned fibers, and hence they have an advantage over extrinsic probe studies. However, birefringence techniques lack molecular specificity, and it is difficult to extract model-independent information. Nevertheless, we have found that measurements of birefringence can play a useful role by providing additional constraints and consistency checks on a proposed model of cross-bridge dynamics.

In Section II of the present paper we review the theory of form birefringence and construct an optical model of muscle. Section III consists of a series of tables in which values are derived for parameters in the optical model. In Section IV we adopt plausible orientational distributions for cross-bridges in the resting, active and rigor states, and compare the predictions of our model with published measurements of birefringence. We conclude that more complete measurements of birefringence could yield a great deal of information about orientations of cross-bridges in the three states. We also investigate the dependence of muscle birefringence on sarcomere length and on disorder in the orientation of the thick and thin filament array.

II. THEORY OF THE FORM BIREFRINGENCE OF MUSCLE

We shall follow the treatment of form birefringence developed by Wiener (1912). A readily accessible discussion of Wiener's theory is contained in the paper by Bragg and Pippard (1953), who studied the form birefringence of hemoglobin crystals. In applying Wiener's theory to muscle, it is important to identify approximations which may limit the validity of the results. Hence we shall outline the theory, starting with the fundamentals, and relegate details of the calculations to an appendix.

Form birefringence occurs in a heterogeneous dielectric medium comprised of two or more linear (i.e., the polarization vector is linearly proportional to the electric field), homogeneous, isotropic dielectric materials. In the case of muscle the principal constituent dielectrics are the thick and thin filaments and the sarcoplasm in which they are immersed. The dielectric constant (or polarizability or refractive index) of these protein filaments is greater than that of the sarcoplasm. The molecular structure of the filaments may lead to some anisotropy in their polarizability, but this anisotropy contributes to the so-called intrinsic birefringence of muscle which must be added to the form birefringence to obtain the total birefringence. In modeling the form birefringence of muscle we shall assume that the thick and thin filaments are composed of a linear, homogeneous, isotropic dielectric material.

On a molecular level the phenomenon of form birefringence is simply the anisotropic shielding of a molecule from the electric field of an incident light wave by the remaining molecules in the system. The anisotropy of the shielding is due to the anisotropy of the macroscopic shapes formed by the remaining molecules. In the case of muscle, a molecule in the interior of a thick filament will experience a larger electric field if an incident field of strength E_o is polarized parallel to the fiber axis rather than perpendicular to it. Formally this anisotropy emerges from the boundary conditions on the electric field at the interfaces of the various constituent dielectrics (see treatment by Born and Wolf [1970]).

To illustrate Wiener's theory we shall calculate the form birefringence of a crude model of muscle, consisting of long parallel cylinders (thick and thin filaments) immersed in a liquid (sarcoplasm). We shall add refinements, notably cross-bridges, later. We assume that the protein cylinders and the sarcoplasm are composed of linear, homogeneous, isotropic dielectric materials, and so the electric field and electric displacement vectors in these materials are related by:

$$\mathbf{D}_s = \epsilon_s \mathbf{E}_s \quad \text{and} \quad \mathbf{D}_f = \epsilon_p \mathbf{E}_f, \tag{1}$$

where the subscripts s and f refer to sarcoplasm and filaments, respectively, and ϵ_s and ϵ_p are the permittivities of the sarcoplasm and protein, respectively. The refractive index is related to the permittivity by

$$n_s^2 = \epsilon_s/\epsilon_o \quad \text{and} \quad n_p^2 = \epsilon_p/\epsilon_o, \tag{2}$$

where ϵ_0 is the permittivity of the vacuum.

To facilitate an optical description of our heterogeneous model for muscle, we define an effective (fictitious) linear and homogeneous medium that is not isotropic. If the incident electric field is polarized parallel or perpendicular to the fiber axis, we define the **E** and **D** fields of the effective medium to be the spatially averaged fields of our heterogeneous model for muscle:

$$\langle \mathbf{E} \rangle = f_s \langle \mathbf{E}_s \rangle + f_f \langle \mathbf{E}_f \rangle \tag{3}$$

$$\langle \mathbf{D} \rangle = n_s^2 \epsilon_o f_s \langle \mathbf{E}_s \rangle + n_p^2 \epsilon_o f_f \langle \mathbf{E}_f \rangle, \tag{4}$$

where the angle brackets $\langle\ \rangle$ denote a spatial average, and the f's are the volume fractions of the dielectric components (here $f_s + f_f = 1$).

This "mean field" or "effective medium" approach requires that the wavelength of the incident light be large compared with the size and spacing of optical inhomogeneities in the medium, a condition which also reduces calculations of form birefringence to problems in electrostatics. In a cross-section of muscle perpendicular to the fiber axis, the thick filaments form a hexagonal lattice with a spacing of 45 nm, i.e., staggered rows of thick filaments are separated by 27.5 nm. Assuming the incident light wave is a helium-neon laser beam, the wavelength in muscle will be 633 nm/1.38 = 459 nm, where 1.38 is the average refractive index of muscle. Hence at any particular time the incident electric field will vary in phase by (45 nm/459 nm) 2π = 35° over three staggered rows of thick filaments and the accompanying interdigitating thin filaments. We shall neglect this variation in phase.

In a cross-section of muscle parallel to the fiber axis, the spacing and lengths of the thick and thin filaments are certainly not less than the wavelength of light; on the contrary, they are 1–2 μm, several times the wavelength of light. We must consider whether these sarcomeric dimensions, in addition to causing an optical diffraction pattern, will thwart our attempt to model muscle with an "effective medium." We will argue that, for light detected on the zero order of the diffraction pattern, the thick and thin filaments can be modeled to a good approximation by infinitely long filaments. Interestingly, the effective medium approach is valid for infinitely long filaments; the problem simply reduces to that of a uniaxial crystal.

Consider an incident beam polarized parallel to the fiber axis. The primary consequence of the finite length of

the thick and thin filaments is that polarization charge will form on their ends. In particular, equal but opposite polarization charges will form on opposite ends of the thick filaments that comprise a single myofibrillar A-band. We must appraise the depolarizing effect of these polarization charges on the field in the A-band (or in the adjacent I-bands). Because the incident electric field varies sinusoidally in time, the charges on opposite ends of the thick filaments will exchange sign at optical frequencies. At time t, the field at a point in the middle of the A-band depends upon the magnitude and sign of the polarization charges on the ends of the thick filaments at the retarded time $t - r/c$, where r is the distance to the polarization charges. If the field at time t in the middle of the A-band is "depolarizing," then points $\lambda/2$ away on either side experience a "polarizing" field due to the polarization charges on the ends of the thick filaments. In general, the A-band (and the adjacent I-bands) consists of alternating strips of axial width $\lambda/2$, which experience opposing effects due to the presence of the polarization charge on the ends of the filaments. It can be shown that the contribution of the polarization charge on the ends of filaments is <1% of the form birefringence of muscle. Therefore we model the thick and thin filaments as infinitely long cylinders, and treat our calculation of the form birefringence of muscle as a problem in electrostatics.

Let us return to the application of Eqs. 3 and 4 to an array of infinitely long filaments. The spatial average operation in Eqs. 3 and 4 is trivial if $\mathbf{E}_s$ and $\mathbf{E}_f$ are uniform; otherwise some method of calculating a spatial average must be devised, perhaps involving an approximation. For example, if the incident field is polarized parallel to the fiber axis, $\mathbf{E}_s$ and $\mathbf{E}_f$ are uniform, and the brackets in Eqs. 3 and 4 can simply be dropped. Indeed, in this case,

$$\langle \mathbf{E}_f \rangle_{para} = \langle \mathbf{E}_s \rangle_{para}, \tag{5}$$

independent of the volume fractions f_s and f_f. Because our effective medium is by definition linear and homogeneous, we can define an effective refractive index for light beams polarized parallel to the fiber axis:

$$n^2_{para} = \frac{\langle \mathbf{D} \rangle_{para}}{\epsilon_o \langle \mathbf{E} \rangle_{para}} = n_s^2 f_s + n_p^2 f_f. \tag{6}$$

If, however, the incident field is polarized perpendicular to the fiber axis, $\mathbf{E}_s$ is not uniform and the values of $\langle \mathbf{E}_s \rangle_{perp}$ and $\langle \mathbf{E}_f \rangle_{perp}$ depend in general on the volume fractions f_s and f_f and on the packing symmetry of the parallel array of protein cylinders. A common approach to this problem is to assume a dilute solution of cylinders ($f_f \ll 1$), and then to make the plausible assumption that the average fields $\langle \mathbf{E}_s \rangle_{perp}$ and $\langle \mathbf{E}_f \rangle_{perp}$ are given by their values in the case in which a field is applied to a single cylinder immersed in an infinite medium of sarcoplasm. Pugh and Pugh (1960) calculate the fields for a single (infinitely long) cylinder immersed in an infinite medium:

$$\mathbf{E}_{sperp} = \mathbf{E}_o + \mathbf{E}_{dipole/meter} \quad \text{and} \quad \mathbf{E}_{fperp} = \mathbf{E}_o/[1 + (\Delta n)(1/2)],$$

where $\mathbf{E}_o$ is the field applied perpendicular to the cylinder axis, and $\mathbf{E}_{dipole/meter}$ is the field in the sarcoplasm due to a polarization dipole moment per unit length on the axis of the cylinder with magnitude

$$\text{dipole/meter} = 2\pi R^2 \epsilon_o E_o (n_p^2 - n_s^2)/(n_p^2 + n_s^2),$$

where R is the radius of the cylinder. The factor (1/2) in the denominator of $\mathbf{E}_{fperp}$ is called the "depolarizing factor" in the radial direction for a cylinder (see Appendix A and Osborn [1945] and Stoner [1945]), and $\Delta n = (n_p^2 - n_s^2)/n_s^2$. Note that the field $\mathbf{E}_{fperp}$ in the cylinder is uniform, so that performing the spatial average of this field is trivial. However, the field $\mathbf{E}_{sperp}$ in the sarcoplasm is the sum of the (uniform) incident field E_o and the nonuniform field $\mathbf{E}_{dipole/meter}$. The average of the dipolar field over the volume of the sarcoplasm vanishes. Hence if, for the moment, we adopt the dilute solution approximation, we have for the spatially averaged fields in the sarcoplasm and cylinders:

$$\langle \mathbf{E}_s \rangle_{perp} = \mathbf{E}_o \quad \text{and} \quad \langle \mathbf{E}_f \rangle_{perp} = \mathbf{E}_o/[1 + (\Delta n)(1/2)]. \tag{7}$$

For a dilute solution of cylinders we can then define an effective refractive index for light beams polarized perpendicular to the fiber axis:

$$n^2_{perp} = \frac{\langle \mathbf{D} \rangle_{perp}}{\epsilon_o \langle \mathbf{E} \rangle_{perp}} = \frac{n_s^2 f_s + n_p^2 f_f/[1 + (\Delta n)(1/2)]}{f_s + f_f/[1 + (\Delta n)(1/2)]}. \tag{8}$$

Using the relation $f_s + f_f = 1$, we can put this expression in the form of Eq. 3 of Bragg and Pippard (1953):

$$n^2_{perp} = n_s^2 + \frac{f_f(n_p^2 - n_s^2)}{1 + f_s(\Delta n)(1/2)}. \tag{9}$$

Notice that as $f_f \to 0$, $n_{perp} \to n_s$, and as $f_s \to 0$, $n_{perp} \to n_p$. Notice also that if the radial depolarizing factor (1/2) is replaced by zero, $n_{perp} \to n_{para}$, as it should because the depolarizing factor in the axial direction for a cylinder is zero. The birefringence of this dilute solution of cylinders is positive:

$$B_{filaments} = n_{para} - n_{perp} > 0, \tag{10}$$

where n_{para} and n_{perp} are given by Eqs. 6 and 8.

The dilute solution approximation requires justification. Rayleigh (1892) presented a rigorous solution for the case of square or rectangular arrays of parallel cylinders. His predicted birefringence for a square array differs by <0.1% from the dilute solution result (Eqs. 6, 8,

and 10) for volume fractions <0.36 (and $n_s \approx 1.35$, $n_p \approx 1.53$). Because the total volume fraction of muscle protein is <0.13, the dilute solution result would be more than adequate for a muscle model employing a square array of cylinders. Stokes (1963) presented without derivation an expression for the birefringence of a hexagonal array of parallel cylinders. The expression seems to include the leading correction provided by Rayleigh's method to the dilute solution result. Stokes' predicted birefringence for a hexagonal array differs by <0.1% from the dilute solution result for volume fractions <0.44. Hence we shall adopt the dilute solution approach.

One noteworthy consequence of the applicability of the dilute solution result is that the ratio of the electric field inside a thick or thin filament to that in the sarcoplasm is independent of the filament volume fraction and the filament packing symmetry. In particular this field ratio is the same throughout the sarcomere, despite the slight variation in volume fraction and packing symmetry which occurs in moving from the overlap region to the H-zone or the Z-band. From Eqs. 3 and 4 it follows that the form birefringence of the muscle filament array depends only on the average filament volume fraction in the sarcomere. Therefore the contribution of the filament array to the form birefringence of an intact muscle fiber should be independent of sarcomere length, because changes in sarcomere length maintain constant sarcomere volume. Of course the orientation of cross-bridges may be different in the overlap and nonoverlap regions of the sarcomere, thus giving rise to some dependence of the birefringence on sarcomere length. We shall come back to this point in Section IV.

To refine our optical model for muscle we must add cross-bridges. We consider a cross-bridge to be comprised of two pieces: the myosin head (S-1), which we model as a spheroid, i.e., an ellipsoid of revolution, and long S-2, which we model as a thin, rodlike, prolate spheroid. Actually we have used depolarizing factors for the S-2 spheroid which are appropriate to a very elongated prolate spheroid, i.e., an infinitely long cylinder. We assume that a universal joint connects S-1 to S-2. Fig. 1 depicts this model of a cross-bridge and parametrizes the orientation of the components with respect to the fiber axis.

It should be emphasized that only the shapes and orientations of S-1 and S-2 in Fig. 1 are relevant to our calculation of the form birefringence of muscle. The size and relative positions are irrelevant. For example, the volume fraction f_1 of S-1 spheroids could equally well consist of twice as many spheroids, each with half the volume, and positioned randomly with respect to the S-2 spheroids and the filament array. Only the axial ratio of the S-1 spheroid (ratio of semiaxis along the axis of revolution to semiaxis normal to the axis of revolution)

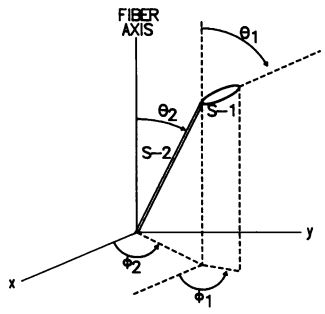

FIGURE 1 Angles defining the orientation of a cross-bridge. The S-1 spheroid is drawn with an axial ratio of 18.5 nm/4.5 nm = 4.1 (see Elliott and Offer [1978]). The ratio of the volume of the S-1 spheroid to the volume of the S-2 cylinder is drawn to be $f_1/f_2 = 0.023/0.009$ (see Table 6). The ratio of the length (major axis) of S-1 to the length of S-2 is drawn to be 18.5 nm/66.2 nm. (For the length of S-1, see Elliott and Offer [1978]. We calculate the length of long S-2 by 0.15 nm per residue times 441 residues for rat myosin; see Strehler et al. [1986].) Only the shapes and orientations of S-1 and S-2 are used in our calculation of birefringence; the size and relative positions are irrelevant.

and the orientations of the spheroids play a role in the calculation. Similarly, as a consequence of our dilute solution approach to the birefringence of the filament array, only the volume fraction f_f of the array is relevant. The radii and number of filaments is irrelevant; there is no distinction between thick and thin filaments.

To include the effect of cross-bridges in the calculations of n_{para} and n_{perp} (Eqs. 6 and 8), we must add terms to the starting Eqs. 3 and 4. We have:

$$\langle \mathbf{E} \rangle = f_s \langle \mathbf{E}_s \rangle + f_f \langle \mathbf{E}_f \rangle + f_1 \langle \mathbf{E}_1 \rangle + f_2 \langle \mathbf{E}_2 \rangle \quad (11)$$

$$\langle \mathbf{D} \rangle = n_s^2 \epsilon_o f_s \langle \mathbf{E}_s \rangle + n_p^2 \epsilon_o [f_f \langle \mathbf{E}_f \rangle + f_1 \langle \mathbf{E}_1 \rangle + f_2 \langle \mathbf{E}_2 \rangle], \quad (12)$$

where f_1 and f_2 are the volume fractions of S-1 and S-2, respectively, and we have taken the refractive index of the protein comprising the cross-bridges to be the same as that of the filaments. The values of the average fields $\langle \mathbf{E}_1 \rangle$ and $\langle \mathbf{E}_2 \rangle$ in S-1 and S-2, respectively, for an incident field polarized parallel or perpendicular to the fiber axis are derived in Appendix A. The results are contained in Eqs. A7 and A8 and pertain to a general spheroid, either S-1 or S-2. We apply the results here:

$$\langle \mathbf{E}_1 \rangle_{para} / \langle \mathbf{E}_s \rangle_{para} = A_1 - (A_1 - B_1) \langle \sin^2 \Theta_1 \rangle \quad (13)$$

$$\langle \mathbf{E}_1 \rangle_{perp} / \langle \mathbf{E}_s \rangle_{perp} = B_1 + (1/2)(A_1 - B_1) \langle \sin^2 \Theta_1 \rangle \quad (14)$$

where Θ_1 is the polar angle describing the orientation of the S-1 spheroid (see Fig. 1), $A_1 = [1 + (\Delta n) L_1]^{-1}$, $B_1 = [1 + (\Delta n) M_1]^{-1}$, $\Delta n = (n_p^2 - n_s^2)/n_s^2$, and L_1 and M_1 are the depolarizing factors of the S-1 spheroid parallel and perpendicular to the axis of revolution, respectively. L_1

and M_1 are determined by the axial ratio of the S-1 spheroid (see Appendix A and Osborn [1945] and Stoner [1945]). Analogous equations hold for the S-2 spheroid; the subscript 1 in Eqs. 13 and 14 is simply replaced with a subscript 2. The angle brackets in $\langle \sin^2 \Theta_1 \rangle$ (and $\langle \sin^2 \Theta_2 \rangle$) in Eqs. 13 and 14 indicate an average over Θ_1 (and Θ_2) according to the orientational distribution appropriate to the state of the muscle fiber: resting, active, or rigor.

The derivation of Eqs. 13 and 14 for the average fields in the cross-bridge employs another dilute solution approximation. We have assumed that the average fields in a cross-bridge spheroid are given by their values in the case in which a field is applied to a single spheroid immersed in an infinite medium of sarcoplasm. The field in a particular cross-bridge may be affected by the proximity of other cross-bridges and by the proximity of the thick and thin filament array. Our approximation neglects such interaction effects. Whereas this approximation is similar to the dilute solution approach used in calculating the average fields in the filament array, the disorder in cross-bridge position and orientation renders the present approximation difficult to evaluate and justify. It seems reasonable to assume that these interaction effects will be small and that they will average to zero over the muscle fiber.

There is one final addition to our optical model for muscle. Some structural protein and other nonsoluble solids in muscle contribute isotropically to the refractive index either because their structures are spherical or because their non-spherical structures are oriented isotropically. We must add another term to Eqs. 11 and 12 to include the contribution of these effectively isotropic structures:

$$\langle \mathbf{E} \rangle = f_s \langle \mathbf{E}_s \rangle + f_f \langle \mathbf{E}_f \rangle + f_1 \langle \mathbf{E}_1 \rangle + f_2 \langle \mathbf{E}_2 \rangle + f_i \langle \mathbf{E}_i \rangle \quad (15)$$

$$\langle \mathbf{D} \rangle = n_s^2 \epsilon_o f_s \langle \mathbf{E}_s \rangle + n_p^2 \epsilon_o [f_f \langle \mathbf{E}_f \rangle + f_1 \langle \mathbf{E}_1 \rangle + f_2 \langle \mathbf{E}_2 \rangle + f_i \langle \mathbf{E}_i \rangle], \quad (16)$$

where we have taken the refractive index of these structures to be n_p. The expression for the average fields $\langle \mathbf{E}_i \rangle$ is taken to be that for a single dielectric sphere immersed in an infinite medium of sarcoplasm.

$$\langle \mathbf{E}_i \rangle_{para} = \langle \mathbf{E}_i \rangle_{perp} = \langle \mathbf{E}_s \rangle / [1 + (\Delta n)(1/3)], \quad (17)$$

where the depolarizing factor for a sphere is 1/3.

We now summarize our procedure for calculating the form birefringence of muscle. The definition of the form birefringence of a muscle fiber is

$$B_{form} = n_{para} - n_{perp}. \quad (18)$$

The effective refractive indexes for light polarized parallel or perpendicular to the fiber axis are defined to be

$$n_{para}^2 = \frac{\langle \mathbf{D} \rangle_{para}}{\epsilon_o \langle \mathbf{E} \rangle_{para}} \quad \text{and} \quad n_{perp}^2 = \frac{\langle \mathbf{D} \rangle_{perp}}{\epsilon_o \langle \mathbf{E} \rangle_{perp}}. \quad (19)$$

Using the definitions of the average fields $\langle \mathbf{E} \rangle$ and $\langle \mathbf{D} \rangle$ in our optical model (see Eqs. 15 and 16), we can write

$$n_{para}^2 = \frac{n_s^2 f_s + n_p^2 (f_f r_{fpara} + f_1 r_{1para} + f_2 r_{2para} + f_i r_{ipara})}{f_s + f_f r_{fpara} + f_1 r_{1para} + f_2 r_{2para} + f_i r_{ipara}} \quad (20)$$

$$n_{perp}^2 = \frac{n_s^2 f_s + n_p^2 [f_f r_{fperp} + f_1 r_{1perp} + f_2 r_{2perp} + f_i r_{iperp}]}{f_s + f_f r_{fperp} + f_1 r_{1perp} + f_2 r_{2perp} + f_i r_{iperp}}. \quad (21)$$

The ratios of the average fields in the thick and thin filament array to those in the sarcoplasm can be written with the help of Eqs. 5 and 7:

$$r_{fpara} = [1 + (\Delta n) L_f]^{-1} \quad \text{and} \quad r_{fperp} = [1 + (\Delta n) M_f]^{-1} \quad (22)$$

where $\Delta n = (n_p^2 - n_s^2)/n_s^2$, and the depolarizing factors for (infinitely long) cylinders parallel and perpendicular to the cylinder axis are $L_f = 0$ and $M_f = 1/2$. The ratios of the average fields in the S-1 spheroids to those in the sarcoplasm can be written with the help of Eqs. 13 and 14:

$$r_{1para} = A_1 - (A_1 - B_1) \langle \sin^2 \Theta_1 \rangle \quad \text{and} \quad r_{1perp} = B_1 + (1/2)(A_1 - B_1) \langle \sin^2 \Theta_1 \rangle, \quad (23)$$

where $A_1 = [1 + (\Delta n) L_1]^{-1}$ and $B_1 = [1 + (\Delta n) M_1]^{-1}$. The depolarizing factors L_1 and M_1 for the S-1 spheroid depend only upon the assumed axial ratio (see Osborn [1945] or Stoner [1945]). The angle brackets in $\langle \sin^2 \Theta_1 \rangle$ represent an average over an assumed orientational distribution for the S-1 spheroids. Analogous equations hold for r_{2para} and r_{2perp}; we have taken for the depolarizing factors $L_2 = 0$ and $M_2 = 1/2$, which are appropriate for a long, rodlike prolate spheroid, i.e., an infinitely long cylinder. Finally the field ratios for the effectively isotropic matter follow from Eq. 17:

$$r_{ipara} = r_{iperp} = [1 + (\Delta n)(1/3)]^{-1}, \quad (24)$$

where we have used the depolarizing factor (1/3) for a sphere.

In Section III we calculate values for the volume fractions in these equations and select literature values for the refractive indexes of sarcoplasm and protein. In Section IV we adopt plausible orientational distributions for the cross-bridges in resting, active and rigor muscle. The final calculations are performed by computer.

III. VALUES FOR PARAMETERS IN THE OPTICAL MODEL OF MUSCLE

We have calculated values for the volume fractions and refractive indexes involved in our optical model of muscle.

Tables 1–6 outline our calculations, including references and consistency checks. The final values are listed in Table 6. The tables are heavily commented and are intended to be self-explanatory.

Most of the data on muscle proteins has come from mammalian skeletal muscle, namely rabbit and rat. The relevant measurements of refractive indexes have been performed on frog skeletal muscle. Clearly the appropriate values for volume fractions and refractive indexes will depend somewhat upon whether rabbit or frog muscle birefringence is being studied, and especially upon whether intact or demembranated muscle is used. The sensitivity of the predicted birefringence to variation in the values of parameters listed in Table 6 is discussed in Section IV.

IV. RESULTS AND DISCUSSION

We now use the optical model developed in Section II to calculate the form birefringence of muscle in the resting, active, and rigor states. The essential quantitative relations of the optical model are contained in Eqs. 18–24. Values for the parameters in the model are listed in Table 6 or appear in Fig. 1. However, we also need plausible descriptions of the orientations of the cross-bridges during the resting, active, and rigor states to evaluate the orientational averages $\langle \sin^2 \Theta_1 \rangle$ and $\langle \sin^2 \Theta_2 \rangle$ for the S-1 and S-2 spheroids (see Eq. 23).

To illustrate the use of the model, we choose orientational distributions for S-1 which are appropriate to a model for cross-bridge dynamics suggested by Huxley and Kress (1985). We could equally well choose orientational distributions appropriate to any other hypothetical model for cross-bridge dynamics and compare the predictions of our model with published measurements of birefringence. The Huxley-Kress model, however, is particularly interesting because it combines into a single picture the information yielded by x-ray studies (e.g., Huxley et al. [1982], Haselgrove and Huxley [1973]), paramagnetic probe studies (e.g., Crowder and Cooke [1987], Cooke et al. [1984]), and optical probe studies (e.g.,

TABLE 1 Composition by weight and volume of 1 g of whole skeletal muscle

Substance	Weight	Specific volume	Volume
	g	*ml/g*	*ml*
Water			
Total	0.80*	1.00	0.80**
Extracellular water	0.13‡	1.00	0.13
Intracellular water	0.67	1.00	0.67**
Solids Total	0.20*	0.73¶	0.146**
Total protein	0.18§	0.73¶	0.131
Soluble protein	0.061‖	0.73¶	0.044
Structural protein	0.119	0.73¶	0.087**
Other solids	0.02	0.73¶	0.015

*See Table 1 (p. 4) of Dubuisson (1954).
‡See Boyle et al. (1941).
§See Table 2 (p. 5) of Dubuisson (1954).
‖See Table 5 (p. 256) of Hanson and Huxley (1957).
¶The specific volume of the thick filament is 0.73 ml/g. See Table 1 of Godfrey and Harrington (1970); we also acknowledge a personal communication from M.E. Rodgers and W.F. Harrington. For convenience we have used 0.73 ml/g as the specific volume for all proteins and solids in skeletal muscle. See also p. 377 of Cohn and Edsall (1943), who cite a value of 0.74–0.75 ml/g for protein in general.
**The volume of 1 g of whole muscle is then 0.80 ml water + 0.146 ml solids = 0.946 ml, which gives a density of 1.057 g/ml, in agreement with the generally quoted value of 1.05–1.06 g/ml. The intracellular volume is 0.67 ml water + 0.146 ml solids = 0.816 ml, and hence the intracellular volume fraction of structural protein is 0.087/0.816 ml = 0.107.

TABLE 2 Intracellular volume fractions of structural proteins

Structural protein	Percent by weight of total	Intracellular volume fraction
Total structural protein	100	0.107*
Actin	22‡	0.024
Troponin	5‡	0.005
Tropomyosin	5‡	0.005
Myosin	43‡	0.046
C-, X-, H-, and M-protein, and creatine phosphokinase	4‡	0.004
Titin	10‡	0.011
Nebulin	5‡	0.005
Subtotal of proteins comprising anisotropic structures	94	0.101
Form-isotropic proteins	6	0.006

*See note ** of Table 1.
‡See Table 8 (p. 138) of Yates and Greaser (1983).

TABLE 3 Contributions of myosin heavy chains (MHC) and light chains (LC) to the molecular weight of myosin

Myosin chain	Molecular weight	Number per myosin molecule	Total contribution to myosin molecular weight
	kD		*kD*
MHC	224*	2	448
A-1 LC	20.7‡	1	20.7
A-2 LC	16.5‡	1	16.5
DTNB LC	19.0‡	2	38.0
Myosin molecule		1	523

*See Strehler et al. (1986).
‡See review by Wagner (1982).

TABLE 4 Contributions of myosin subfragments to the molecular weight of myosin

Subfragment (No. per myosin molecule)	Total MHC contribution	Total LC contribution	Subfragment molecular weight
	kD	*kD*	*kD*
S-1 (2)	192*	75.2‡	267
S-2 (2)	102*		102
LMM (1)	154*		154
Myosin molecule (1)	448	75.2	523

*See Strehler et al. (1986).
‡See Table 3.

Burghardt et al. [1983], Yanagida [1981]). An excellent review of the probe studies has recently appeared (Thomas [1987]). Huxley and Kress (1985) suggested that two types of binding of myosin heads to actin occur in the active state of muscle: (*a*) a strong binding in which S-1 is rotationally immobile, and which is responsible for tension generation and is similar to the binding in rigor, and (*b*) a weak binding in which S-1 is nearly rotationally free. Evidence for such a weakly attached state has been provided by a paramagnetic probe study of S-1 cross-linked to actin. Svensson and Thomas (1986) reported microsecond rotational motion of S-1 in a cross-linked actomyosin preparation during steady-state ATPase activity. They concluded that "myosin heads may rotate on actin after all, although it seems likely that they are predominantly in a weakly attached state that precedes force generation."

Huxley and Kress further suggested that during isometric contraction roughly 20% of myosin heads are strongly bound and 80% are weakly bound. Huxley and Kress designed their model to be consistent with two types of x-ray data taken during isometric contraction: (*a*) observations of equatorial reflections (Haselgrove and Huxley [1973]) indicate that up to 90% of myosin heads have moved out to the actin filaments, and (*b*) the intensities of actin layer line reflections indicate that probably no more than 30% of myosin heads are attached to actin in a specific orientation (Huxley et al. [1982]). The model is also designed to be consistent with paramagnetic probe studies (Cooke et al. [1982]) which indicate that in isometric contraction only 20% of myosin heads are rotationally immobile, whereas 80% are oriented nearly isotropically. It is worth noting here that not all probe studies report the 20/80% figures (Thomas [1987]). For example, one optical probe study (Burghardt et al. [1983]) suggests that roughly 65% of S-1 has a specific orientation in active muscle.

TABLE 5 Intracellular volume fractions of myosin subfragments

Subfragment	Fraction of myosin molecular weight	Volume fraction
Myosin molecule	1.00	0.046*
S-1	0.51‡	0.023
S-2	0.20‡	0.009
LMM	0.29‡	0.014

*See Table 2.
‡See Table 4.

Cross-bridge orientations in the optical model

Employing the model proposed by Huxley and Kress, we have adopted the following orientational distributions for S-1. In the active state under conditions of full overlap between the thick and thin filaments, the 20% of S-1 which are strongly bound make a specific angle Θ_1 with the fiber axis, whereas the remaining 80% possess an orientational distribution which is either "uniform" (equal weighting in Θ_1 between 0 and 180°) or isotropic in Θ_1. Note that a "uniform" distribution of Θ_1 for weakly bound S-1 means that the average $\langle \sin^2 \Theta_1 \rangle$ in Eq. 23 is equal to 1/2, whereas a truly isotropic distribution yields an average of 2/3.

$$\langle \sin^2 \Theta_1 \rangle_{\text{uniform}} = (1/\pi) \int_0^{\pi} (\sin^2 \Theta_1)\, d\Theta_1 = 1/2$$

$$\langle \sin^2 \Theta_1 \rangle_{\text{isotropic}} = (1/4\pi) \int_0^{\pi} \int_0^{2\pi} (\sin^2 \Theta_1) \sin \Theta_1\, d\phi_1\, d\Theta_1 = 2/3.$$

We have considered a uniform distribution in token recognition of the steric hindrance which may limit the azimuthal rotational freedom of S-1. However, we have plotted the results in Fig. 2 for both uniform and isotropic distributions. In the rigor state of muscle we assume that all S-1 are oriented at the same Θ_1 as the strongly bound S-1 in active muscle.

In resting muscle we assume that the orientational distribution of S-1 is either uniform (equal weighting in Θ_1) or isotropic in Θ_1. This assumption is motivated by the finding that paramagnetic probes are oriented nearly isotropically in resting muscle (Thomas et al. [1980], Thomas and Cooke [1980]). It is important to remember,

TABLE 6 Values for parameters in the optical model of muscle

Volume fraction of S-1	$f_1 = 0.023$*
Volume fraction of S-2	$f_2 = 0.009$*
Volume fraction of filaments	$f_f = 0.069$‡
Volume fraction of form-isotropic solids	$f_i = 0.024$§
Volume fraction of sarcoplasm	$f_s = 0.875$‖
Total volume fraction	1.000
Refractive index of sarcoplasm	$n_s = 1.35$¶
Effective refractive index of hydrated protein	$n_p = 1.53$**

*See Table 5.

‡f_f = 0.101 (volume fraction of protein comprising anisotropic structures, from Table 2).
$-f_1 - f_2$.

§f_i = 0.006 (volume fraction of form-isotropic structural protein, from Table 2).
+0.018 (volume fraction of other form-isotropic solids; calculated from Table 1 as 0.015 ml other solids/0.816 ml intracellular volume).

‖Calculated from Table 1 as (0.67 ml intracellular water + 0.044 ml soluble protein)/0.816 ml intracellular volume.

¶The value n_s = 1.35 is calculated using Table 1 and the value 0.185 ml/g for the specific refractive increment of protein (see Barer and Joseph [1954] and Davies et al. [1954]). The calculation is n_s = 1.333 (refractive index of water) + 0.185 ml/g × 0.061 g soluble protein/(0.67 ml intracellular water + 0.044 ml soluble protein) = 1.349. Note that the mean refractive index of a muscle fiber can be calculated in a similar manner: n_{fiber} = 1.333 + 0.185 ml/g × 0.20 g solids/0.816 ml intracellular vol = 1.378. This value is identical to the mean refractive index measured by Huxley and Niedergerke (1958) for eight fibers immersed in their neutralized protein solution.

**See Bragg and Pippard (1953) and p. 406 of Barer and Joseph [1954].

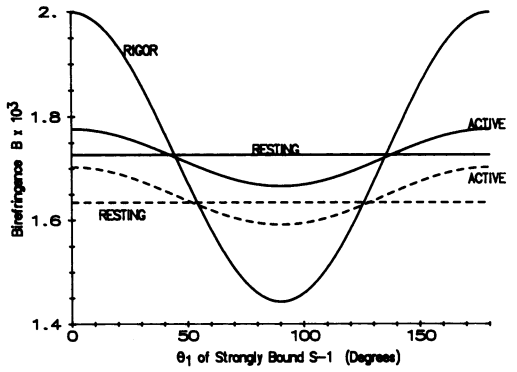

FIGURE 2 Calculated form birefringence of muscle in the resting, active, and rigor states as a function of the angle Θ_1 which strongly bound S-1 makes with the fiber axis. The axial ratio of the S-1 spheroid has been taken to be 4.1. Resting birefringence is independent of Θ_1 because we assume that no cross-bridges are bound to actin, and that the unattached S-1 are oriented with a uniform distribution of Θ_1 between 0 and 180° (*solid line*) or oriented isotropically (*dashed line*). Active birefringence is calculated assuming that 20% of S-1 are strongly bound at a single value of Θ_1, whereas the remaining 80% are oriented with a uniform distribution of Θ_1 between 0 and 180° (*solid line*) or oriented isotropically (*dashed line*). Rigor birefringence is calculated assuming 100% of S-1 are strongly bound at a single value of Θ_1. We have assumed that S-2 makes an angle Θ_2 = 0° with the fiber axis in the resting state, but that Θ_2 = 8° in the active and rigor states.

however, that probe studies measure the angle between the fiber axis and a specific axis of the probe, and that the probe axis is not in general parallel to the long axis of S-1. Mendelson and Wilson (1982) have shown that in cases in which the probe axis is not parallel to the axis of S-1 there may be partial order in the orientations of S-1 even though the observed probe orientations are nearly isotropic. For the moment we shall ignore this possibility and simply take a uniform or isotropic distribution for the orientations of S-1 in resting muscle.

We have adopted an orientational distribution for S-2 which is simple but somewhat arbitrary. In resting muscle we have taken Θ_2 to be 0°, indicating that S-2 lies on the surface of the thick filament. In active and rigor muscle we have taken Θ_2 to be 8°, roughly the angle required for long S-2 (66.2 nm in length) to bridge the surface to surface distance (9.5 nm) between thick and thin filaments.

Comparison with published measurements of birefringence

There is some evidence from paramagnetic probe studies (Thomas and Cooke [1980], Thomas et al. [1975]) that strongly bound S-1 makes an angle $\Theta_1 \approx 68°$ with the fiber axis. It is interesting to investigate whether the predictions of our model in conjunction with published measurements of muscle birefringence can provide independent support for this value of Θ_1. We have plotted in Fig. 2 our calculated form birefringence of muscle in the resting, active, and rigor states as a function of Θ_1 of strongly bound S-1. The general magnitude of the predicted values is in agreement with observed values of muscle birefringence. For example, Eberstein and Rosenfalck (1963) reported a value of $1.92 \pm 0.03 \times 10^{-3}$ for intact frog fibers at rest, and a value 8.2 ± 1.2% lower for isometrically contracting fibers. Taylor (1976) reported values of $1.67 \pm 0.05 \times 10^{-3}$ for resting and $1.46 \pm 0.08 \times 10^{-3}$ for rigor fibers from rabbit psoas muscle which was treated with triton and glycerol solutions. It should be noted that our model does not include a contribution from intrinsic birefringence, as will be discussed later.

Notice in Fig. 2 that for $50° \leq \Theta_1 \leq 130°$ the predicted birefringence decreases during activation of muscle and continues to decrease during the transition to rigor. Several groups of researchers have reported decreases in birefringence in the resting to active and resting to rigor transitions (Eberstein and Rosenfalck [1963], Taylor [1976], Yanagida [1976], Irving and Peckham [1986], Irving et al. [1987]). Unfortunately birefringence has not been measured in the sequence of transitions, resting to active to rigor, in the same muscle preparation. Recent

preliminary reports (Irving and Peckham [1986], Irving et al. [1987]) indicate that rigor birefringence may be slightly greater than in isometric contraction, but full details of these measurements have not been published. It is clear from Fig. 2 that our orientational distributions for S-1 lead to a conflict between a value of $\Theta_1 = 68°$ for strongly bound S-1 and a birefringence in rigor which is higher than that of active muscle. In fact, our orientational distributions for S-1 are incompatible with values for rigor and active birefringence which are approximately equal and are also substantially less than that for resting birefringence. It would clearly be useful to perform measurements of birefringence in resting, active, and rigor states in intact fibers and in demembranated fibers.

If indeed rigor birefringence is comparable with or greater than active birefringence, we may want to reconsider our uniform or isotropic distribution for S-1 in resting muscle. If we assume that the orientational distribution of S-1 in resting muscle has considerably more order than the paramagnetic probe studies indicate (Thomas et al. [1980], Thomas and Cooke [1980]), we can raise the predicted birefringence of resting muscle. It is noteworthy that fluorescent probe studies (Wilson and Mendelson [1983]) have indeed indicated the presence of some cross-bridge order in resting muscle. Cantino and Squire (1986) presented a model for resting muscle based on electron microscope images of rapidly frozen frog fibers. In their model S-1 makes an angle with the fiber axis of $\Theta_1 = 20$–$40°$. A value of $\Theta_1 = 30°$ leads to a predicted birefringence of resting muscle of 1.87×10^{-3} (compare with Fig. 2). Note that now a value of $\Theta_1 \approx 50°$ for strongly bound S-1 leads to predicted values for rigor and active birefringence which are comparable, and yet both values are substantially less than that for resting muscle. Another consequence of a value of $\Theta_1 \approx 50°$ for strongly bound S-1 is that measurements of birefringence would be insensitive to the relative proportions of myosin heads that are strongly or weakly bound in active muscle.

In our discussion thus far we have modeled S-1 as a spheroid with axial ratio 4.1 and have assumed that it maintains this shape in the resting, contracting, and rigor states. We have considered only the effects of rotations of this spheroid. There is some evidence that during the power stroke S-1 may undergo a conformational change involving a rotation of the portion of S-1 distal to actin, whereas the portion of S-1 proximal to actin remains rigidly attached (see review by Cooke [1986], also Highsmith and Eden [1986]). Whereas a shape change in S-1 will affect our predicted birefringence for the active and rigor states, it will not lead to values which are substantially less than the predicted resting value unless substantial order of cross-bridges is assumed in the resting state, as in the model of Cantino and Squire described above. This is an interesting point, but strong statements regarding the orientation of resting cross-bridges cannot be made until more extensive muscle birefringence data is available.

Dependence on sarcomere length

Our model can be used to predict the dependence of the form birefringence of muscle on sarcomere length in the resting, active, and rigor states. In the case of intact fibers, changes in sarcomere length maintain constant sarcomere volume. We pointed out in Section II that for constant sarcomere volume our model predicts a contribution of the filament array to the birefringence which is independent of the sarcomere length. However, the orientation of the cross-bridges will certainly depend upon the degree of filament overlap in active or rigor muscle, leading to some sarcomere length dependence of the birefringence.

The predictions of our model are plotted in Fig. 3. The solid lines are calculated assuming that the S-1 in the nonoverlap region have an orientational distribution which is uniform in Θ_1 between 0 and 180°. The dashed lines are calculated assuming a truly isotropic distribution for the nonoverlap S-1, illustrating the effect of greater rotational mobility for these myosin heads than for the weakly bound (active state) or unattached (resting state) heads in the overlap region. It should be noted that the curves for the active state in Fig. 3 lie closer to the resting

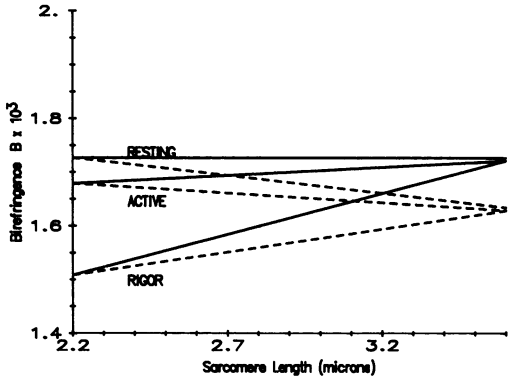

FIGURE 3 Calculated form birefringence of muscle in the resting, active, and rigor states as a function of sarcomere length. Values for parameters in the model are the same as those in Fig. 2, but we have chosen $\Theta_1 = 70°$ for strongly bound S-1. The weakly bound or unattached S-1 in the overlap region are oriented with a uniform distribution of Θ, between 0 and 180°. The unattached S-1 in the nonoverlap region are oriented with a uniform distribution of Θ_1 between 0 and 180° (*solid lines*) or oriented isotropically (*dashed lines*). We have taken a sarcomere length of 2.2 μm to be 100% overlap and 3.6 μm to be 0% overlap of thick and thin filaments.

curves than the rigor curves because we assume only 20% of S-1 are strongly bound in active muscle. If we assume, for example, that 80% of S-1 are strongly bound in the active state, then the active curves would lie proportionately closer to the rigor curves.

Eberstein and Rosenfalck (1963) measured a linear decrease in birefringence accompanying activation of intact fibers as the sarcomere length was increased. Their data is consistent with the difference of either set of resting and active curves in Fig. 3. Unfortunately they did not report absolute values of birefringence for the resting and active states, so their difference data cannot distinguish between the two models for nonoverlap S-1. There seem to be no published data on intact fibers which can directly test the predicted curves. Data on demembranated fibers would suffice if carefully corrected for the variation in volume fractions as the sarcomere length is varied.

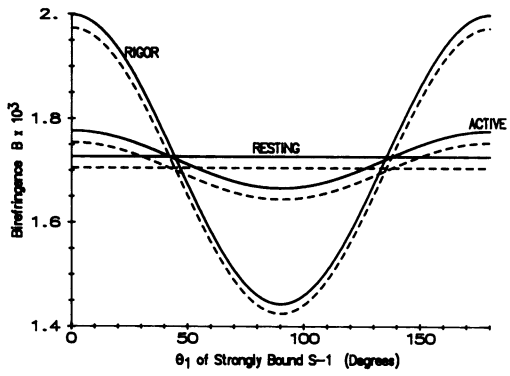

FIGURE 4 Calculated form birefringence of muscle as a function of Θ_1 in the presence and absence of myofilament disorder. The solid curves are identical to the solid curves in Fig. 2. The dashed curves include the effect of myofilament disorder; the filaments are assumed to point with equal probability in a cone of half-angle 7.5°.

Effect of myofilament orientational disorder

The array of thick and thin filaments in a muscle fiber is not perfectly oriented along a single direction, particularly in demembranated fibers. Thomas and Cooke (1980) reported that paramagnetic probes in rigor fibers (glycerinated rabbit psoas) were highly ordered, but nevertheless were oriented in a cone with a half-angle of ~7.5°. This slight disorder may represent a true range of attachment angles with which S-1 may bind to actin, or it may simply reflect some orientational disorder of the myofilament array. We have used our model for muscle to investigate the effect of myofilament orientational disorder on the predicted form birefringence in the resting, active, and rigor states.

We have assumed that portions of the filament array in a fiber point with equal probability in a cone of half-angle $\Delta\Theta_c$ centered on the average orientation $\Theta = 0^0$. The effect of this disorder is discussed quantitatively in Appendix B. The predicted birefringence is plotted in Fig. 4 for no disorder ($\Delta\Theta_c = 0^0$, solid lines) and for disorder comparable with that reported by Thomas and Cooke (1980) for paramagnetic probes in rigor fibers ($\Delta\Theta_c = 7.5°$, dashed lines). The dominant effect is a slight decrease in birefringence contributed by the filament array; the disorder in the orientation of S-1 and S-2 contributes a much smaller amount.

Intrinsic birefringence

Our present model does not include a contribution from intrinsic birefringence. Imbitition studies (see the analysis by Sato et al. [1975] of the imbibition data of Noll and Weber [1935]) suggest that the intrinsic component may comprise 30% of the total birefringence of skeletal muscle. The imbibition technique requires fixation of the muscle to achieve reproducible birefringence changes as the imbibing medium is cycled; the fixation procedure generally alters the birefringence (for example see Taylor [1976]). Our model predicts a value for the form birefringence of resting muscle of 1.73×10^{-3} (uniform, see Fig. 2) or 1.63×10^{-3} (isotropic) which is roughly 90% of the measured value for the total birefringence, 1.92×10^{-3}, for intact frog fibers (Eberstein and Rosenfalck [1963]).

An intrinsic contribution to muscle birefringence could come from an intrinsic anisotropy in the polarizability of the filament array or of the cross-bridges. A contribution from the filament array would result to first approximation in a single additive constant augmenting the values predicted by our model for the resting, active, and rigor states. However, an intrinsic anisotropy in the polarizabilities of S-1 or S-2 could result in different additive constants for the three states with their different orientational distributions for cross-bridges. A satisfying treatment of these intrinsic contributions will have to wait for a more detailed knowledge of the intrinsic polarizability matrix of S-1 and S-2.

Sensitivity of the predicted birefringence to values for parameters in the model

The equations of the model (Eqs. 18–24) are not transparent functions of the various parameters in the model. We have therefore tabulated the effects on the predicted birefringence of small variations in the model parameters about their standard values listed in Table 6. Since the effects of variations in the volume fraction and axial ratio of S-1 will depend upon the assumed orientational distri-

TABLE 7 Sensitivity of the predicted birefringence to values for parameters in the model

	ΔB_{rest}(isotropic S-1)*	$\Delta B_{rigor}(\Theta_1 = 70°)$‡
	%	%
$\Delta f_f = \pm 5\%$	±4	±4
$\Delta f_1 = \pm 5\%$	±0.1	±0.5
$\Delta R = \pm 30$§	—	±1
$\Delta\Theta_1 = \pm 10°$	—	±4
$\Delta f_2 = \pm 5\%$	±0.5	±0.6
$\Delta\Theta_2 = \pm 8°$	−0.3	±0.7
$\Delta f_i = \pm 5\%$	±0.1	±0.1
$\Delta n_s = \pm 0.3\%$	±5	±5
$\Delta n_p = \pm 0.7\%$	±12	±12

*Using the parameter values listed in Table 6, taking $\Theta_2 = 0°$, and using an isotropic orientational distribution for S-1 yields $B_{rest} = 1.63 \times 10^{-3}$. See dashed line in Fig. 2.

‡Using the parameter values listed in Table 6, taking $\Theta_2 = 8°$, using an axial ratio for S-1 of $R = 4.1$, and taking $\Theta_1 = 70°$ for all S-1 yields $B_{rigor} = 1.51 \times 10^{-3}$. See rigor curve in Fig. 2.

§The variation in axial ratio is $R = 2.87$–5.33.

bution of S-1, we list in Table 7 the effects on the predicted birefringence of two states of muscle. First we investigate the resting state with an isotropic distribution of S-1; this state should be insensitive to variations in the parameters associated with S-1. As a second state we choose the rigor state with all S-1 oriented at $\Theta_1 = 70°$; this state should be reasonably sensitive to S-1 parameters.

The variations in parameters listed in Table 7 reflect our rough estimates of the uncertainties in the parameters. When the volume fraction of a particular protein is increased, the sarcoplasm volume fraction is decreased by an equal amount; the total volume fraction must, of course, equal one. It is clear from Table 7 that the calculated birefringence is most sensitive to the refractive indexes for protein and sarcoplasm and to the volume fraction of the filament array. In addition the birefringence is sensitive to the value of Θ_1 in the rigor state. In general, variations in Θ_1 are important when the average value of $\sin^2\Theta_1$ is significantly different from the isotropic value of 2/3, i.e., when S-1 contributes significantly to the birefringence. This last point is precisely the reason that we feel studies of muscle birefringence can yield significant information about the structure and orientation of cross-bridges in resting, active, and rigor muscle.

APPENDIX A. CALCULATION OF THE RATIO OF THE ELECTRIC FIELD INSIDE A SPHEROID TO THE APPLIED FIELD OUTSIDE THE SPHEROID

Consider a single spheroid of protein (modeling S-1 or S-2) oriented at angles Θ and ϕ with respect to the z-axis (fiber axis) and with refractive index n_p. See, for example, Fig. 1. The spheroid is immersed in an infinite medium of sarcoplasm with refractive index n_s.

If we apply an external electric field $\mathbf{E}_o$ along the direction of the axis of revolution, the field inside the spheroid will be uniform and given by (see Stratton [1941])

$$\mathbf{E}_{para} = \frac{\mathbf{E}_o}{1 + (\Delta n)L} = A\mathbf{E}_o, \tag{A1}$$

where $\Delta n = (n_p^2 - n_s^2)/n_s^2$, L is the depolarizing factor along the axis of revolution, and $A = [1 + (\Delta n)L]^{-1}$. Although the field in the sarcoplasm is not uniform, its spatial average is just equal to the applied field, $\langle \mathbf{E}_s \rangle = \mathbf{E}_o$. If the external field is directed perpendicular to the axis of revolution, the field is again uniform and given by

$$\mathbf{E}_{perp} = \frac{\mathbf{E}_o}{1 + (\Delta n)M} = B\mathbf{E}_o, \tag{A2}$$

where M is the depolarizing factor perpendicular to the axis of revolution, and $B = [1 + (\Delta n)M]^{-1}$. Again the spatial average of the field in the sarcoplasm is equal to the applied field. Osborn (1945) and Stoner (1945) give analytic expressions for L and M as functions of the axial ratio $R = a/b$, where a is the semiaxis along the axis of revolution, and b is the semiaxis perpendicular to the axis of revolution.

If the external field is applied along some arbitrary direction rather than along one of the principal axes of the spheroid, then by superposition the field inside the spheroid is still uniform but is not necessarily parallel to the applied field since, in general, $L \neq M$. The spatial average of the field in the sarcoplasm is by superposition still equal to the applied field.

For example, if the external field is applied along the fiber axis, we can calculate the field inside the spheroid using the Euler angle formalism described by Rose (1957). We have

$$\mathbf{E}_{para} = \begin{bmatrix} E_{xpara} \\ E_{ypara} \\ E_{zpara} \end{bmatrix} = \underline{\underline{R}}_z(-\phi)\underline{\underline{R}}_{y'}(-\Theta) \cdot \begin{bmatrix} B & 0 & 0 \\ 0 & B & 0 \\ 0 & 0 & A \end{bmatrix} \underline{\underline{R}}_{y'}(\Theta)\underline{\underline{R}}_z(\phi) \begin{bmatrix} 0 \\ 0 \\ E_o \end{bmatrix}, \tag{A3}$$

where $\mathbf{E}_o = E_o\mathbf{e}_z = \begin{bmatrix} 0 \\ 0 \\ E_o \end{bmatrix}$.

The product of rotation matrices $\underline{\underline{R}}_{y'}(\Theta)\underline{\underline{R}}_z(\phi)$ projects the applied field onto the principal axes of the spheroid, and the product $\underline{\underline{R}}_z(-\phi)\underline{\underline{R}}_{y'}(-\Theta)$ projects the total electric field in the spheroid back onto the fiber axes. According to Rose (1957) the rotation matrices are

$$\underline{\underline{R}}_{y'}(\Theta) = \begin{bmatrix} \cos\Theta & 0 & -\sin\Theta \\ 0 & 1 & 0 \\ \sin\Theta & 0 & \cos\Theta \end{bmatrix}$$

$$\text{and } \underline{\underline{R}}_z(\phi) = \begin{bmatrix} \cos\phi & \sin\phi & 0 \\ -\sin\phi & \cos\phi & 0 \\ 0 & 0 & 1 \end{bmatrix}. \tag{A4}$$

Multiplying the matrices we have

$$\mathbf{E}_{\text{para}} = E_o \begin{bmatrix} (A - B) & \sin\Theta\cos\Theta\cos\phi \\ (A - B) & \sin\Theta\cos\Theta\sin\phi \\ A - & (A - B)\sin^2\Theta \end{bmatrix}. \quad \text{(A5)}$$

If the external field is applied perpendicular to the fiber axis, e.g., along the x-axis, we calculate in a similar way:

$$\mathbf{E}_{\text{perp}} = E_o \begin{bmatrix} B + (A - B)\sin^2\Theta\cos^2\phi \\ (A - B)\sin^2\Theta\sin\phi\cos\phi \\ (A - B)\sin\Theta\cos\Theta\cos\phi \end{bmatrix}. \quad \text{(A6)}$$

We shall assume that cross-bridges in a muscle fiber are oriented with an effectively continuous and uniform distribution in azimuthal angle ϕ. Hence our results for a spheroid modeling some portion of a cross-bridge should be averaged over ϕ. Eqs. A5 and A6 become

$$\mathbf{E}_{\text{para}}/\mathbf{E}_o = A - (A - B)\sin^2\Theta \quad \text{(A7)}$$

$$\mathbf{E}_{\text{perp}}/\mathbf{E}_o = B + (1/2)(A - B)\sin^2\Theta, \quad \text{(A8)}$$

because the components of the field inside the spheroid which are normal to the applied field average to zero. Eqs. A7 and A8 are discussed in Section II as Eqs. 13 and 14 and later as Eq. 23.

APPENDIX B. EFFECT OF MYOFILAMENT ORIENTATIONAL DISORDER ON THE CALCULATED BIREFRINGENCE

Suppose the thick and thin filaments exhibit a distribution of orientations $(\Delta\Theta, \Delta\phi)$ with respect to the average direction of the fiber axis, the (unprimed) z-axis ($\Theta = 0$). This orientational disorder will affect the contributions of the filament array (Eq. 22) and the S-1 and S-2 spheroids (Eq. 23) to the form birefringence of muscle. Let us rewrite Eq. 22 for the filaments so that it is formally similar to Eq. 23 for the spheroids:

$$r_{\text{fpara}} = A_f - (A_f - B_f)\sin^2\Theta_f$$
$$\text{and} \quad r_{\text{fperp}} = B_f + (1/2)(A_f - B_f)\sin^2\Theta_f, \quad \text{(B1)}$$

where $A_f = [1 + (\Delta n)L_f]^{-1}$, $B_f = [1 + (\Delta n)M_f]^{-1}$, and the depolarizing factors for (infinitely long) cylinders are $L_f = 0$ and $M_f = 1/2$. Without disorder we take $\Theta_f = 0$ so that Eq. B1 reduces to Eq. 22. To account for the effect of disorder, we must replace $\sin^2\Theta_f$ in Eq. B1 and $\sin^2\Theta_1$ (or $\sin^2\Theta_2$) in Eq. 23 with values of $\sin^2\Theta$ which have been averaged over the distribution of orientational disorder.

Let us assume that the thick and thin filaments are oriented with equal probability in a cone of half-angle $\Delta\Theta_c$ centered on the average direction of the filaments $\Theta = 0$ (or $\Delta\Theta = 0$, $\Delta\phi = 0$). Then the value of $\sin^2\Theta$ in Eqs. B1 and 23 must be replaced by its average over the solid angle of the cone:

$$\sin^2\Theta \rightarrow \frac{(1/4\pi)\int_0^{\Delta\Theta_c}\int_0^{2\pi}[\sin^2\Theta']\sin(\Delta\Theta)\,d(\Delta\Theta)\,d(\Delta\phi)}{(1/4\pi)\int_0^{\Delta\Theta_c}\int_0^{2\pi}\sin(\Delta\Theta)\,d(\Delta\Theta)\,d(\Delta\phi)}, \quad \text{(B2)}$$

where $\sin^2\Theta'$ is a function of its value $\sin^2\Theta$ without disorder and of the local deviation $(\Delta\Theta, \Delta\phi)$ of the filaments from the average direction $\Theta = 0$. We can evaluate $\sin^2\Theta'$ if we first note that $\sin^2\Theta = x^2 + y^2$ where (x, y, z) is a point on the unit sphere, and then note that $\sin^2\Theta' = (x')^2 + (y')^2$ where (x', y', z') is the same point referred to coordinate axes which have been rotated by the Eulerian angles $(\Delta\Theta, \Delta\phi)$. Hence we have the relation:

$$\begin{bmatrix} x' \\ y' \\ z' \end{bmatrix} = \begin{bmatrix} \sin\Theta'\cos\phi' \\ \sin\Theta'\sin\phi' \\ \cos\Theta' \end{bmatrix} = \underline{\underline{R}}_{y'}(\Delta\Theta)\underline{\underline{R}}_z(\Delta\phi)\begin{bmatrix} \sin\Theta\cos\phi \\ \sin\Theta\sin\phi \\ \cos\Theta \end{bmatrix}$$
$$= \underline{\underline{R}}_{y'}(\Delta\Theta)\underline{\underline{R}}_z(\Delta\phi)\begin{bmatrix} x \\ y \\ z \end{bmatrix}, \quad \text{(B3)}$$

where the rotation matrices $\underline{\underline{R}}_{y'}(\Delta\Theta)$ and $\underline{\underline{R}}_z(\Delta\phi)$ are given in Appendix A. After some tedious algebra, Eq. B3 yields the relation

$$\begin{aligned} \sin^2\Theta' = {} & [\cos^2(\Delta\Theta)\cos^2(\Delta\phi) + \sin^2(\Delta\phi)]\sin^2\Theta\cos^2\phi \\ & + [\cos^2(\Delta\Theta)\sin^2(\Delta\phi) + \cos^2(\Delta\phi)]\sin^2\Theta\sin^2\phi \\ & + \sin^2(\Delta\Theta)\cos^2\Theta \\ & - 2[1 - \cos^2(\Delta\Theta)]\sin(\Delta\phi)\cos(\Delta\phi)\sin^2\Theta \\ & \cdot \sin\phi\cos\phi \\ & - 2\sin(\Delta\Theta)\cos(\Delta\Theta)\sin(\Delta\phi)\sin\Theta\cos\Theta\sin\phi \\ & - 2\sin(\Delta\Theta)\cos(\Delta\Theta)\cos(\Delta\phi)\sin\Theta\cos\Theta\cos\phi. \quad \text{(B4)} \end{aligned}$$

The average over $\Delta\phi$ in Eq. B2 takes the last three lines of the expression in Eq. B4 to zero. Performing the average over $\Delta\Theta$, Eq. B2 becomes

$$\sin^2\Theta \rightarrow (1/2)[\cos(\Delta\Theta_c) + \cos^2(\Delta\Theta_c)]\sin^2\Theta + (2/3) - (1/3)[\cos(\Delta\Theta_c) + \cos^2(\Delta\Theta_c)]. \quad \text{(B5)}$$

The substitution indicated in Eq. B5 must be made in Eq. 23 for the S-1 and S-2 spheroids before the average is performed over the orientational distributions of the cross-bridges indicated by the angle brackets $\langle\,\rangle$. The substitution in Eq. B1 for the filaments consists only of the second line of Eq. B5 because $\sin^2\Theta_f = 0$. The dashed line in Fig. 4 was calculated using these substitutions with $\Delta\Theta_c = 7.5°$.

This work was supported by United States Public Health Service/ National Institutes of Health grant AM12803 awarded to Dr. Carlson and Muscular Dystrophy Association postdoctoral fellowships awarded to Dr. Haskell.

Received for publication 18 April 1988 and in final form 24 March 1989.

REFERENCES

Barer, R., and S. Joseph. 1954. Refractometry of living cells. *Q. J. Microscop. Sci.* 95:399–423.

Born, M., and E. Wolf. 1970. Principles of Optics. Fourth ed. Section 14.5.2. Pergamon Press, Oxford.

Boyle, P. J., E. J. Conway, F. Kane, and H. L. O'Reilly. 1941. Volume of interfibre spaces in frog muscle and the calculation of concentrations in the fibre water. *J. Physiol. (Lond.)* 99:401–414.

Bragg, W. L., and A. B. Pippard. 1953. The form birefringence of macromolecules. *Acta Crystallogr.* 6:865–867.

Burghardt, T. P., T. Ando, and J. Borejdo. 1983. Evidence for cross-bridge order in contraction of glycerinated skeletal muscle. *Proc. Natl. Acad. Sci. USA.* 80:7515–7519.

Cantino, M., and J. Squire. 1986. Resting myosin cross-bridge configuration in frog muscle thick filaments. *J. Cell Biol.* 102:610–618.

Cohn, E. J., and J. T. Edsall. 1943. Proteins, Amino Acids and Peptides As Ions and Dipolar Ions. Hafner Publishing Co., Inc., New York.

Cooke, R. 1986. The mechanism of muscle contraction. *CRC Crit. Rev. Biochem.* 21:53–118.

Cooke, R., M. S. Crowder, and D. D. Thomas. 1982. Orientation of spin labels attached to cross-bridges in contracting muscle fibres. *Nature (Lond.).* 300:776–778.

Cooke, R., M. S. Crowder, C. H. Wendt, V. A. Barnett, and D. D. Thomas. 1984. Muscle cross-bridges: do they rotate? *In* Contractile Mechanisms in Muscle. G. H. Pollack and H. Sugi, editors. Plenum Publishing Corp., New York. 413–423.

Crowder, M. S., and R. Cooke. 1987. Orientation of spin-labeled nucleotides bound to myosin in glycerinated muscle fibers. *Biophys. J.* 51:323–333.

Davies, H. G., M. H. F. Wilkins, J. Chayen, and L. F. La Cour. 1954. The use of the interference microscope to determine dry mass in living cells and as a quantitative cytochemical method. *Q. J. Microscop. Sci.* 95:271–304.

Dubuisson, Marcel. 1954. Muscular Contraction. Charles C. Thomas Publisher, Springfield, IL.

Eberstein, A., and A. Rosenfalck. 1963. Birefringence of isolated muscle fibres in twitch and tetanus. *Acta Physiol. Scand.* 57:144–166.

Elliott, A., and G. Offer. 1978. Shape and flexibility of the myosin molecule. *J. Mol. Biol.* 123:505–519.

Godfrey, J. E., and W. F. Harrington. 1970. Self-association in the myosin system at high ionic strength. I. Sensitivity of the interaction to pH and ionic environment. *Biochemistry.* 9:886–893.

Hanson, J., and H. E. Huxley. 1957. Quantitative studies on the structure of cross-striated myofibrils. II. Investigations by biochemical techniques. *Biochim. Biophys. Acta.* 23:250–260.

Haselgrove, J. C., and H. E. Huxley. 1973. X-Ray evidence for radial cross-bridge movement and for the sliding filament model in actively contracting skeletal muscle. *J. Mol. Biol.* 77:549–568.

Highsmith, S., and D. Eden. 1986. Myosin subfragment 1 has tertiary structural domains. *Biochemistry.* 25:2237–2242.

Huxley, A. F., and R. Niedergerke. 1958. Measurement of the striations of isolated muscle fibres with the interference microscope. *J. Physiol. (Lond.).* 144:403–425.

Huxley, H. E., and M. Kress. 1985. Crossbridge behaviour during muscle contraction. *J. Muscle Res. Cell Motil.* 6:153–161.

Huxley, H. E., A. R. Faruqi, M. Kress, J. Bordas, and M. H. J. Koch. 1982. Time-resolved x-ray diffraction studies of the myosin layer-line reflections during muscle contraction. *J. Mol. Biol.* 158:637–684.

Irving, M., and M. Peckham. 1986. Birefringence as a probe of cross-bridge orientation in demembranated muscle fibres of frog and rabbit. *J. Physiol. (Lond.).* 377:95P.

Irving, M., M. Peckham, and M. A. Ferenczi. 1987. Birefringence transients induced by caged-ATP photolysis in demembranated rabbit muscle fibres. *Biophys. J.* 51:3a. (Abstr.)

Mendelson, R. A., and M. G. A. Wilson. 1982. Three-dimensional disorder of dipolar probes in a helical array: application to muscle cross-bridges. *Biophys. J.* 39:221–227.

Noll, D., and H. H. Weber. 1935. Polarisationoptik und molekularer Feinbau der Q-abschnitte des Froschmuskels. *Pfluegers Arch. Gesamte Physiol. Menschen. Tiere.* 235:234–246.

Osborn, J. A. 1945. Demagnetizing factors of the general ellipsoid. *Phys. Rev.* 67:351–357.

Pugh, E. M., and E. W. Pugh. 1960. Principles of Electricity and Magnetism. Section 5.8. Addison-Wesley Publishing Co., Reading, MA. 150.

Rayleigh, J. W. S. 1892. On the influence of obstacles arranged in rectangular order upon the properties of a medium. *Philos. Mag.* 34:481–502.

Rose, M. E. 1957. Elementary Theory of Angular Momentum. John Wiley & Sons, New York. 65.

Sato, H., G. W. Ellis, and S. Inoue. 1975. Microtubular origin of mitotic spindle form birefringence. *J. Cell Biol.* 67:501–517.

Stokes, A. R. 1963. The Theory of the Optical Properties of Inhomogeneous Materials. Section 4.3. E. & F. N. Spon Limited, London.

Stoner, E. C. 1945. The demagnetizing factors for ellipsoids. *Philos. Mag.* 36:803–821.

Stratton, J. A. 1941. Electromagnetic Theory. McGraw-Hill Book Co., New York.

Strehler, E. E., M. Strehler-Page, J. Perriard, M. Periasamy, and B. Nadal-Ginard. 1986. Complete nucleotide and encoded amino acid sequence of a mammalian myosin heavy chain gene. Evidence against intron-dependent evolution of the rod. *J. Mol. Biol.* 190:291–317.

Svensson, E. C., and D. D. Thomas. 1986. ATP induces microsecond rotational motions of myosin heads crosslinked to actin. *Biophys. J.* 50:999–1002.

Taylor, D. L. 1976. Quantitative studies on the polarization optical properties of striated muscle. I. Birefringence changes of rabbit psoas muscle in the transition from rigor to relaxed state. *J. Cell Biol.* 68:497–511.

Thomas, D. D. 1987. Spectroscopic probes of muscle cross-bridge rotation. *Annu. Rev. Physiol.* 49:691–709.

Thomas, D. D., and R. Cooke. 1980. Orientation of spin-labeled myosin heads in glycerinated muscle fibers. *Biophys. J.* 32:891–906.

Thomas, D. D., J. C. Seidel, J. S. Hyde, and J. Gergely. 1975. Motion of subfragment-1 in myosin and its supramolecular complexes: saturation transfer electron paramagnetic resonance. *Proc. Natl. Acad. Sci. USA.* 72:1729–1733.

Thomas, D. D., S. Ishiwata, J. C. Seidel, and J. Gergely. 1980. Submillisecond rotational dynamics of spin-labeled myosin heads in myofibrils. *Biophys. J.* 32:873–890.

Wagner, P. D. 1982. Preparation and fractionation of myosin light chains and exchange of the essential light chains. *Methods Enzymol.* 85:72–81.

Wiener, O. 1912. Die theorie des mischkorpers fur das feld der stationaren stromung. *Abh. Sachs. Ges. Wiss.* 32:509–604.

Wilson, M. G. A., and R. A. Mendelson. 1983. A comparison of order and orientation of cross-bridges in rigor and relaxed muscle fibres using fluorescence polarization. *J. Muscle Res. Cell Motil.* 4:671–693.

Yanagida, T. 1976. Birefringence of glycerinated crab muscle fiber under various conditions. *Biochim. Biophys. Acta.* 420:225–235.

Yanagida, T. 1981. Angles of nucleotides bound to cross-bridges in glycerinated muscle fiber at various concentrations of ϵ-ATP, ϵ-ADP, and ϵ-AMPPNP detected by polarized fluorescence. *J. Mol. Biol.* 146:539–560.

Yates, L. D., and M. L. Greaser. 1983. Quantitative determination of myosin and actin in rabbit skeletal muscle. *J. Mol. Biol.* 168:123–141.